

DC Electrical Resistivity Studies in YBCO/BZT Composites

A REPORT SUBMITTED TO
DEPARTMENT OF PHYSICS
NATIONAL INSTITUTE OF TECHNOLOGY, ROURKELA

BY

Rasmita Das

M.Sc Physics

Roll No. - 409PH2088

NIT Rourkela

Under the supervision of
Prof. D. Behera
Department of Physics,



NIT, Rourkela

NATIONAL INSTITUTE OF TECHNOLOGY, ROURKELA



NATIONAL INSTITUTE OF TECHNOLOGY, ROURKELA

CERTIFICATE

This is to certify that the thesis entitled is “DC electrical resistivity studies of YBCO/BZT composite” submitted by Miss Rasmita das in partial fulfillment for the requirement for the award of degree of Master of science degree in physics at NIT, Rourkela is an authentic work carried out by her under my supervision and guidance in low temperature lab of Department of physics.

To the best of my knowledge, the matter embodied in the thesis has not been submitted to any other university/Institute for the award of my degree.

Prof. D. Behera

Department of Physics,

NIT, Rourkela

ACKNOWLEDGEMENT

On the submission of my thesis report titled "DC electrical resistivity studies of YBCO/BZT composite" I would like to thank my guide **Prof. D. Behera** for his patience and his helpful discussion with me during the course of my work in last one year. I would like to thank **Ms. Arpna Kujur** and **Ms. Mousumibala Sahoo** for sharing ideas with me and taking part in my project work. Finally I would like to extend my gratitude towards my Family and all my friends who supported me in my work.

Rasmita Das

ABSTRACT

Bulk YBCO sample is prepared using chemical route method. BZT is used as composite because its properties can be utilized for pinning effect that enhances critical current density. The sample is characterized by the ρ vs. T measurement performed by FOUR PROBE METHOD. Data are collected by computer controlled programming and analyzed for different behaviors. SEM is done to study the grain morphology. It is found that by increase in the weight percentage of BZT in the sample, the transition temperature decreases and from the SEM images, the grains become elongated in sizes. This elongation is advantageous for pinning purpose.

Contents

1. Introduction

1.1 General remarks

1.1.1 Type-I superconductors

1.1.2 Type-II superconductors

1.1.3 Critical current density

1.2 High temperature superconductors: $\text{YBa}_2\text{Cu}_3\text{O}_{7-\delta}$ material

1.2.1 Crystallographic aspects

1.2.2 Anisotropy of YBCO material

2. Micro structural & Electric transport techniques

2.1 SEM (Scanning electron microscope)

2.2 Four probe method

3. Experimental

4. Results & Discussion

5. Conclusions

6. References

Chapter I

1. Introduction

1.1 General remarks:

For a material to be considered a superconductor it has to exhibit two distinctive properties:-

1. The electrical resistivity in superconductors is zero for temperatures below a certain temperature T_c . So, one can apply dc electrical current without losses. In superconductors, the carriers are coupled forming Cooper pairs which are not scattered & therefore zero resistance is obtained. The condensate that results from this coupling is represented by a wave function (ψ) that varies in distances given by the coherence length ξ (T).
2. The applied magnetic field is completely expelled from the interior of the superconducting specimen at temperature below the critical temperature T_c . Cooper pairs circulating at the surface of the sample that are able to screen the external magnetic field generate the expulsion. These currents penetrate into the sample in a distance characterized by the penetration length, λ (T), leading to an exponential decay of the magnetic field from the interior of a superconducting sample is known as the Meissner-Ochsenfeld effect. Temperature dependence of electrical resistivity of the oxide superconductor: $\text{YBa}_2\text{Cu}_3\text{O}_{7-\delta}$; (b) Exclusion of a weak, external magnetic field from the interior of the superconducting material has been shown.

Superconductors are of two types: type I & type II superconductors, whether the Ginzburg- Landau parameter k is smaller or larger than $\sqrt{1/2}$ respectively. The Ginzburg- Landau parameter k is defined as:

$$k = \lambda/\xi$$

Where " λ " describes the penetration depth of the magnetic field inside the superconductor & ξ is the characteristic length over which the cooper pair density increases from 0 to its maximum value n . For a type-I superconductor $k < \sqrt{1/2}$, whereas for a type-II superconductor, $k > 1/\sqrt{1/2}$.

1.1.1 TYPE-I SUPERCONDUCTOR:

All the elemental superconductors exhibit flux expulsion up to a critical magnetic field (H_C) beyond which flux penetrates the material and drives it to normal state. This type of superconductors is called of type-I.As explained by BCS theory, Type-I superconductivity is exhibited by materials with a regularly structured lattice. This allows electrons to be coupled over a relatively large distance (compared to the size of an atom). These pairings are called Cooper pairs.

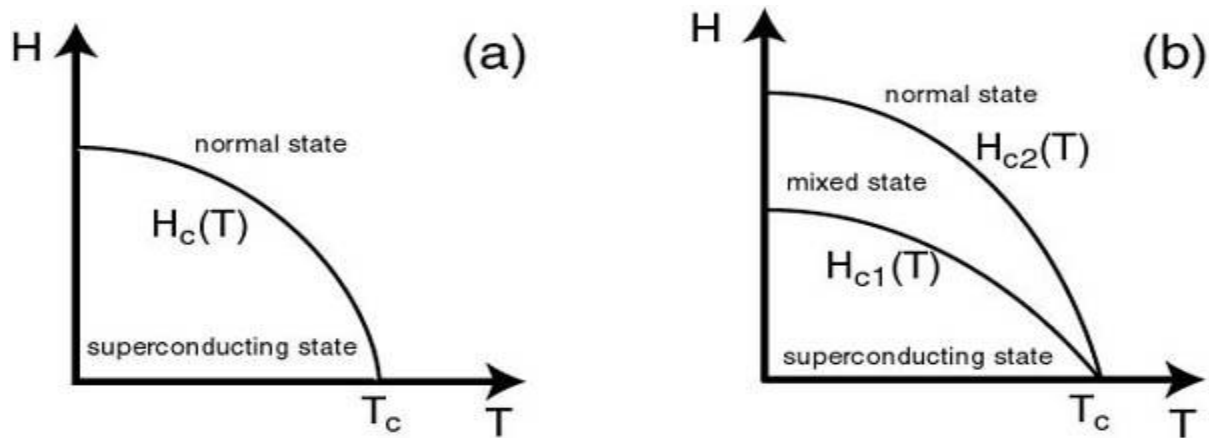


Fig.1: Magnetic phase diagram (H (T)) for a) Type–I superconductors: one critical field H_c exists; b) Type-II superconductors: where two critical fields exist (Lower critical field (H_{c1}) & upper critical field (H_{c2}))

1.1.2 Type-II superconductor

This type of superconductivity is exhibited by transition metals with high values of the electrical resistivity in the normal state i.e. The electronic mean free path in the normal state is short. The figure below shows the behavior of magnetic field to material.

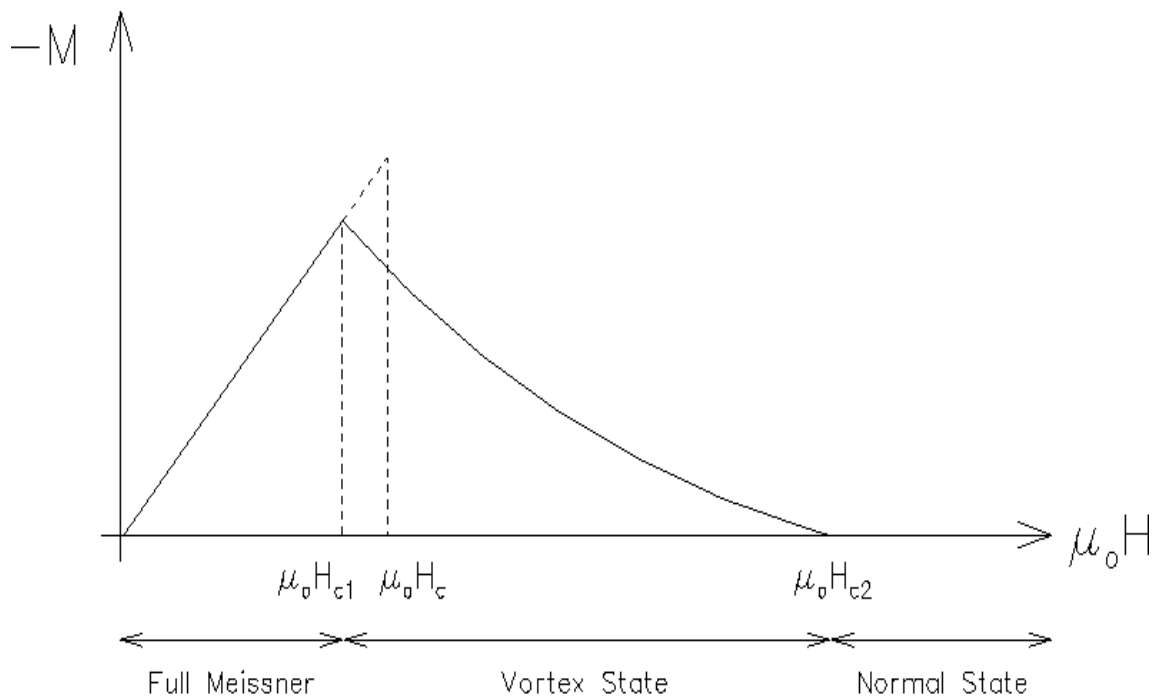


Figure .2 **M –H graph showing the different state of a type-II superconductor**

1.1.3 CRITICAL CURRENT DENSITY:

It corresponds to the maximum current which can transport the material without dissipation.

The critical current density of oxide superconductors, as in the case of conventional superconductors, depends on the applied magnetic field & the temperature at which is measured. By increasing the temp. & the applied magnetic field, the critical current density diminishes. In addition high- T_c superconductors are highly anisotropic, thus the critical current density depends on the crystallographic direction in which is applied.

In the mixed state, when an external current density j flows along a superconducting sample, the flux lines start to move under the action of the Lorentz force ($F_L = j \times B$). The movement of flux lines causes the appearance of voltage. When the flux moves at the velocity of v , an electric field E is created in the direction of the current as $E = v \times B$ giving rise to ohmic losses. In order to recover the situation, at which the desired superconducting property of dissipation free- current flow is lost, the flux lines have to be fixed to pinning centers in such a way that $v=0$. The force that holds the core of the flux lines at the pinning centers is called pinning force (F_P) & it allows the system to sustain the Lorentz force between the flux lines & the current with flux motion & dissipation. If the Lorentz force equals the F_P , the depinning critical current density j_{dp} is achieved & the flux lines start to move producing dissipation. In conventional type-II superconductors, the critical current density can be associated to j_{dp} .

Pinning centers in a superconductor result from structural in-homogeneities in the material that yield a local reduction in the order parameter. Therefore the vortex can reduce its energy when positioned on a pinning center. Thus a superconductor free of defects, in the mixed state, has a critical current density $j_c = 0$. Pinning centers should be on the scale of the coherence length ξ to be effective, i.e. in the nanometer range in the case of high- T_c

superconductors. Typical pinning centers found in high temperature superconductor materials are: twin boundaries, dislocations, oxygen vacancies.

The study of the transport properties especially in the region of transition temperature T_c is a tool of studying the characteristics of the superconducting phase. Transport and magnetic properties of the granular system such as YBCO, has drawn attention for the intrinsic properties due to the grains and the extrinsic properties due to grain boundaries. The mesoscopic inhomogeneities such as grain boundaries, cracks, voids etc. having much larger length-scale than the superconducting coherence length ξ and being temperature independent are expected to influence the R-T characteristics. These inhomogeneities dominate the region where zero resistance state is approached. The microscopic inhomogeneities such as structural (twin boundaries, stacking faults) and chemical imperfections (oxygen deficiencies etc.) inside the grains occur in a length-scale smaller than the mesoscopic inhomogeneities, but still larger than ξ . The temperature dependent resistivity of the composite system depends on the connectivity of the grains. It has been claimed that for non-superconducting inclusions to be effective as pinning centers, their size should be of the order of the coherence length. These defects with size in the range of few times of coherence length have been found to act as a means to inhibit vortex motion, which results in the significant enhancement of J_c at high temperatures and applied magnetic fields. We found that nano-sized particles of $BaTiO_3$ incorporated in YBCO superconductors have both inter- and intra-grain modifications. It also signifies the decreasing metallicity of the composites. The broadening of peak in resistivity slope marks the modification of intergranular properties.

It was shown by MacManus et al. [3] that, inclusions of BZO particles of dimensions in the 10-100 nm range could result in a significant improvement of dc properties of YBCO. Very

steep pinning potentials of BZO inclusions and an improvement of the critical current density, J_c have been registered by Ciontea et al. [4] and Pompeo et al [5]. BZO being a dielectric material particularly fills the inter-granular spaces and mechanical and electrical properties of superconductor. In these composites T_c is observed to be limited to change within 1K near 92K in the sample. The normalized resistance behavior shows the sample characteristics and metallicity decreases with BZO addition. In this paper, we report that nano-sized particles of $BaZr_{0.1}Ti_{0.9}O_3$ (BZT) incorporated in YBCO superconductors have both inter- and intra-grain modifications. The coexistence of superconductivity and ferroelectrics has been analyzed through dc electrical resistivity analysis for the samples with different wt. % of BZT content, i.e. combined effect of BZO and $BaTiO_3$.

1.2 HIGH- T_c SUPERCONDUCTOR: $YBa_2Cu_3O_{7-\delta}$ Material

The $YBa_2Cu_3O_{7-\delta}$ material was discovered by P.Chu in 1987 & its T_c is $\approx 91K$. Is the first high T_c superconductor discovered whose critical temp. T_c was above the liquid nitrogen temperature, thus opening the path to many low cost applications.

1.2.1 Crystallographic aspects:

The structure of a high- T_c superconductor is closely related to perovskite structure, and the structure of these compounds has been described as a distorted, oxygen deficient multi-layered perovskite structure. One of the properties of the crystal structure of oxide superconductors is an alternating multi-layer of CuO_2 planes with superconductivity taking place between these layers. The more layers of CuO_2 the higher T_c . This structure causes a large anisotropy in normal conducting and superconducting properties, since electrical currents are carried by holes induced in the oxygen sites of the CuO_2 sheets.

Yttrium barium copper oxide, often abbreviated YBCO, is a crystalline chemical compound with the formula $\text{YBa}_2\text{Cu}_3\text{O}_7$. This material, a famous "high-temperature superconductor", achieved prominence because it was the first material to achieve superconductivity above the boiling point of nitrogen (77 K). YBCO crystallizes in a defect perovskite structure consisting of layers. The boundary of each layer is defined by planes of square planar CuO_4 units sharing 4 vertices (figure 2). The planes can sometimes be slightly puckered perpendicular to these CuO_2 planes are CuO_4 ribbons sharing 2 vertices. The yttrium atoms are found between the CuO_2 planes, while the barium atoms are found between the CuO_4 ribbons and the CuO_2 planes. This structural feature is illustrated in the figure to the right.

Although $\text{YBa}_2\text{Cu}_3\text{O}_7$ is a well-defined chemical compound with a specific structure and stoichiometry, materials with less than seven oxygen atoms per formula unit are non-stoichiometric compounds. The structure of these materials depends on the oxygen content. This non-stoichiometry is denoted by the $\text{YBa}_2\text{Cu}_3\text{O}_{7-x}$ in the chemical formula. When $x = 1$, the O (1) sites in the Cu (1) layer are vacant and the structure is tetragonal. The tetragonal form of YBCO is insulating and does not super conduct. Increasing the oxygen content slightly causes more of the O (1) sites to become occupied. For $x < 0.65$, Cu-O chains along the b -axis of the crystal are formed. Elongation of the b -axis changes the structure to orthorhombic, with lattice parameters of $a = 3.82$, $b = 3.89$, and $c = 11.68 \text{ \AA}$. Optimum superconducting properties occur

when $x \sim 0.07$ and all of the O (1) sites are occupied with few vacancies.

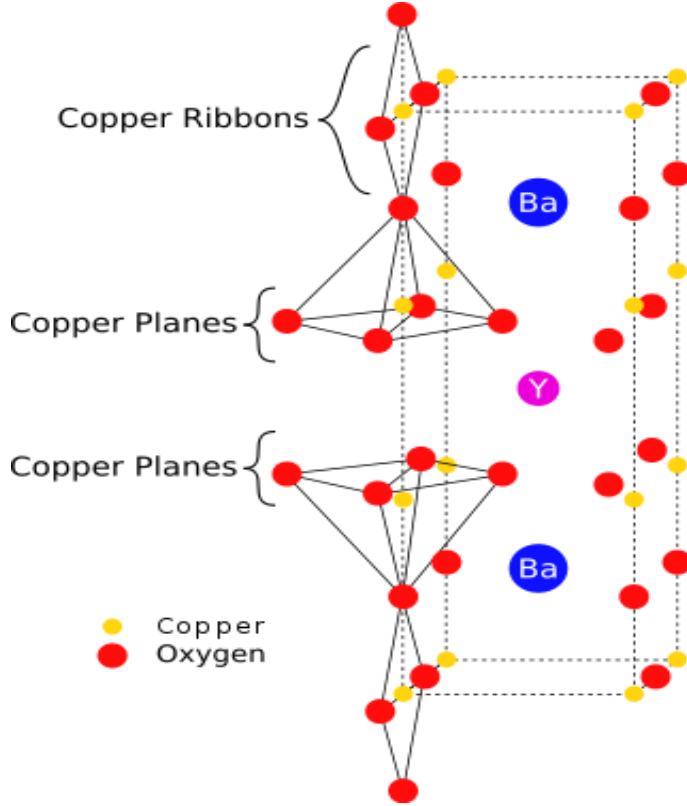


Figure.3 Structure of YBCO in tetragonal phase

1.2.2 Anisotropy of YBCO materials:

Another important aspect of $\text{YBa}_2\text{Cu}_3\text{O}_{7-\delta}$ material is that, like the other cuprates has an isotropic behavior, as a consequence of its crystalline structure that is reflected in the directional dependence of λ , ξ & H_{c2} . The anisotropy of these parameters is remarkable between the c-direction & the a or b direction, while the anisotropy between the a & b direction is small & can be neglected in most cases. The anisotropy of HTS materials can be described using Ginzburg-Landau theory that introduces a different effective mass of the hole carriers in different directions. The effective mass in the ab-plane is denoted m_{ab} & along c- axis m_c . The anisotropy

is described by the parameter γ , defined as $\gamma = (m_c/m_{ab})^{1/2} = H_{c2}^{ab}/H_{c2}^c$ with $\gamma > 1$. The value for YBCO lies between 5 & 8. The large value of Ti & Bi compounds indicate a high anisotropy. As, YBCO has a relatively small γ value which means that it is less anisotropic.

The anisotropy of high- T_C superconductors is related to their layered structure & long separation between the CuO_2 planes when compared to ξ_c . YBCO is the less anisotropic high- T_c superconductor because on one side the distances between CuO_2 planes is only $d \approx 8 \text{ \AA}$ & on the other side the CuO chain have metallic conductivity & the superconductivity is induced by proximity effect. In contrast Bi, Ti compounds are more anisotropic because the charge reservoir blocks are insulators & the distance is much larger than the respective value of $2\xi_c$. The anisotropy of the effective mass γ in these compounds drive, as a consequence, to an anisotropy in the critical current density, i.e. $j_c^{ab} \gg j_c^c$.

2. Micro-structural & Four probe techniques:

2.1 SEM (scanning electron microscope):

The scanning electron microscope (SEM) is a type of electron microscope that images the sample surface by scanning it with a high-energy beam of electrons. The types of signals produced by an SEM include secondary electrons, back-scattered electrons (BSE), characteristic X-rays, light (cathode luminescence), specimen current and transmitted electrons. Secondary electron detectors are common in all SEMs, but it is rare that a single machine would have detectors for all possible signals. The signals result from interactions of the electron beam with atoms at or near the surface of the sample.

SEM Back-scattered electrons (BSE) are beam electrons that are reflected from the sample by elastic scattering. BSE are often used in analytical SEM along with the spectra made

from the characteristic X-rays. Because the intensity of the BSE signal is strongly related to the atomic number (Z) of the specimen, BSE images can provide information about the distribution of different elements in the sample can produce very high-resolution images of a sample surface, revealing details about less than 1 to 5 nm in size. Due to the very narrow electron beam, SEM micrographs have a large depth of field yielding a characteristic three-dimensional appearance useful for understanding the surface structure of a sample.

Characteristic X-rays are emitted when the electron beam removes an inner shell electron from the sample, causing a higher energy electron to fill the shell and release energy. These characteristic X-rays are used to identify the composition and measure the abundance of elements in the sample.

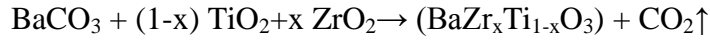
2.2 ELECTRIC TRANSPORT CHARACTERIZATION (FOUR PROBE METHOD):

The determination of the resistance as the ratio of the voltage signal (measured with a Keithley nano voltmeter) and the current source (Keithley). The four-contact configuration is fundamental because it enables to minimize the contribution of spurious voltage signals due to current contacts. The error due to the voltage contact contribute is also minimized because the input impedance of the nanovoltmeter is $1\text{G}\Omega$ or higher, so the current flowing in voltage circuit between the sample and the nanovoltmeter is at least 10^{-9} times lower than the applied current.

3. EXPERIMENTAL PROCEDURE

$\text{YBa}_2\text{Cu}_3\text{O}_{7-\delta}$ superconductor powders were synthesized from organic solution dissolved with Y_2O_3 , BaCO_3 , and CuO powders. A stoichiometric amount of the cationic ratio of Y: Ba: Cu= 1:2:3 was stirred in 2-Methyl ethanol and mixed well for 12 hrs. This solution was dried and evaporated at $70\text{-}80^\circ\text{C}$ until well mixed powders were obtained. Then the powders were grinded

for 1hr, and then were calcined at 900^oc for 12 hrs. The pellets were made from the calcined powders, sintered at 920^oc for 12 hrs and annealed at 500^oC for 8 hrs. BaZr_xTi_{1-x}O₃ (BZT) ceramics were prepared by solid state reaction method using the following chemical reaction: -



High purity starting materials (BaCO₃, TiO₂, and ZrO₂) were weighed and wet mixed with distilled water. After drying, the powders were calcinated at 1000^oc for 2 hrs. Superconductor YBCO-ferroelectric BaZr_xTi_{1-x}O₃ composites were made from a mixture of pre-reacted YBCO powder and BaZr_xTi_{1-x}O₃ powder. A series of polycrystalline composite samples of (1-x) YBCO + xBaZr_{0.1}Ti_{0.9}O₃ (where x = 1.0, 5.0 and 10.0) were grinded and pressed into pellets. The composite pellets were sintered at 920⁰ C for 12 h and then cooled to 500⁰ C, where they were kept for 5h in an oxygen atmosphere for oxygen annealing. The grain morphology of the samples was analyzed by scanning electron microscopy (Model No JSM-6480 LV, Make JEOL) and temperature dependent resistance was measured using standard four-probe techniques with a nanovoltmeter (Keithley-2182 A), Current source (Keithley 6221) and Temperature controller (Lakeshore 332).

4. RESULTS AND DISCUSSION

4.1 DC ELECTRICAL RESISTIVITY

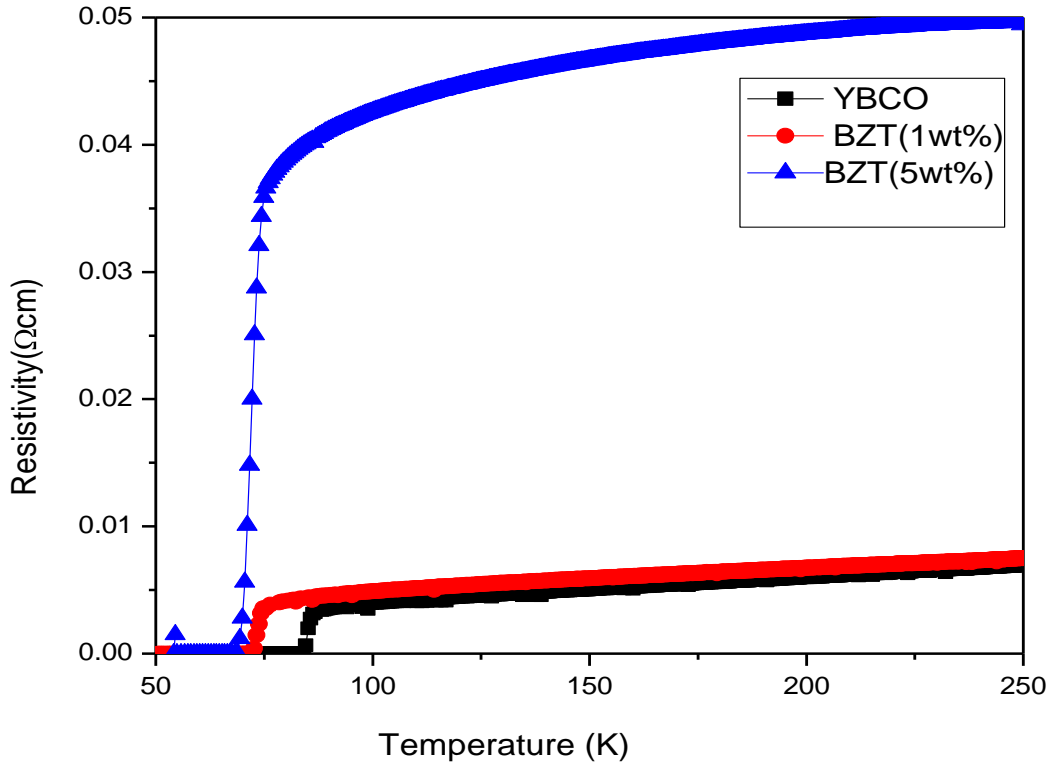


Figure.4 Temperature dependence of the resistivity for YBCO + xBZT composites(x = 0, 1, and 5 wt. %).

It is observed that T_c is affected due to BZT addition. The plot exhibits two different regimes. The one is corresponding to the normal state that shows a metallic behavior (above $2T_c$). The normal resistivity is found to be linear from room temperature to a certain temperature. The other is the region characterized by the contribution of Cooper pairs fluctuation to the conductivity above T_c . This is mainly due to the increasing rate of pair formation on decreasing the temperature. From the R-T plot it is observed that the metallicity of the composites decreasing.

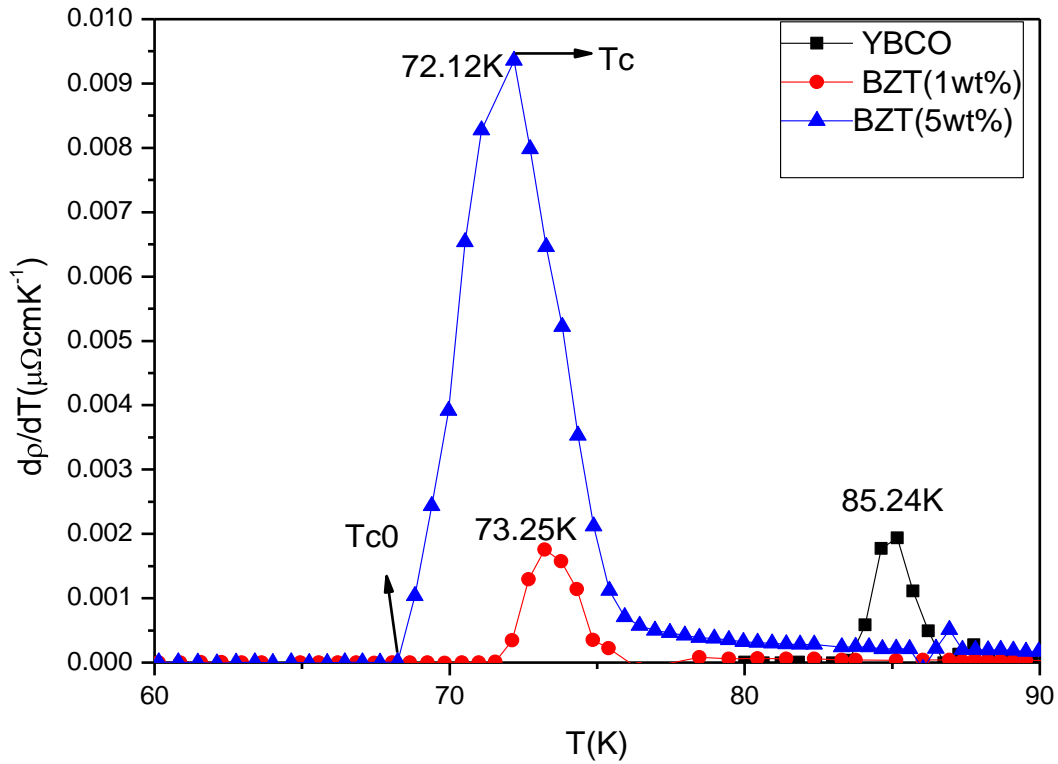


Fig.5 Temperature derivative of resistivity of YBCO + $x\text{BaZr}_{0.1}\text{Ti}_{0.9}\text{O}_3$ composites ($x = 0.0, 1.0, 5.0$ wt. %).

T_c value decreases with increase in $\text{BaZr}_{0.1}\text{Ti}_{0.9}\text{O}_3$ wt. % in the composites and affect the system various critical temperatures observed from the composites through incorporation of nanoparticles of $\text{BaZr}_{0.1}\text{Ti}_{0.9}\text{O}_3$ as listed in table and the temperature derivative of resistivity curves (Fig. 5) shows a decreasing trend with increasing wt. % of $x\text{BaZr}_{0.1}\text{Ti}_{0.9}\text{O}_3$. The broadening of peak in resistivity slope marks the modification of intergranular properties.

BZT (wt. %)	T_{c0} (K)	T_c (K)
0.0	81.15	85.24
1.0	71.79	73.23
5.0	68.17	72.09

4.2 Grain Morphology

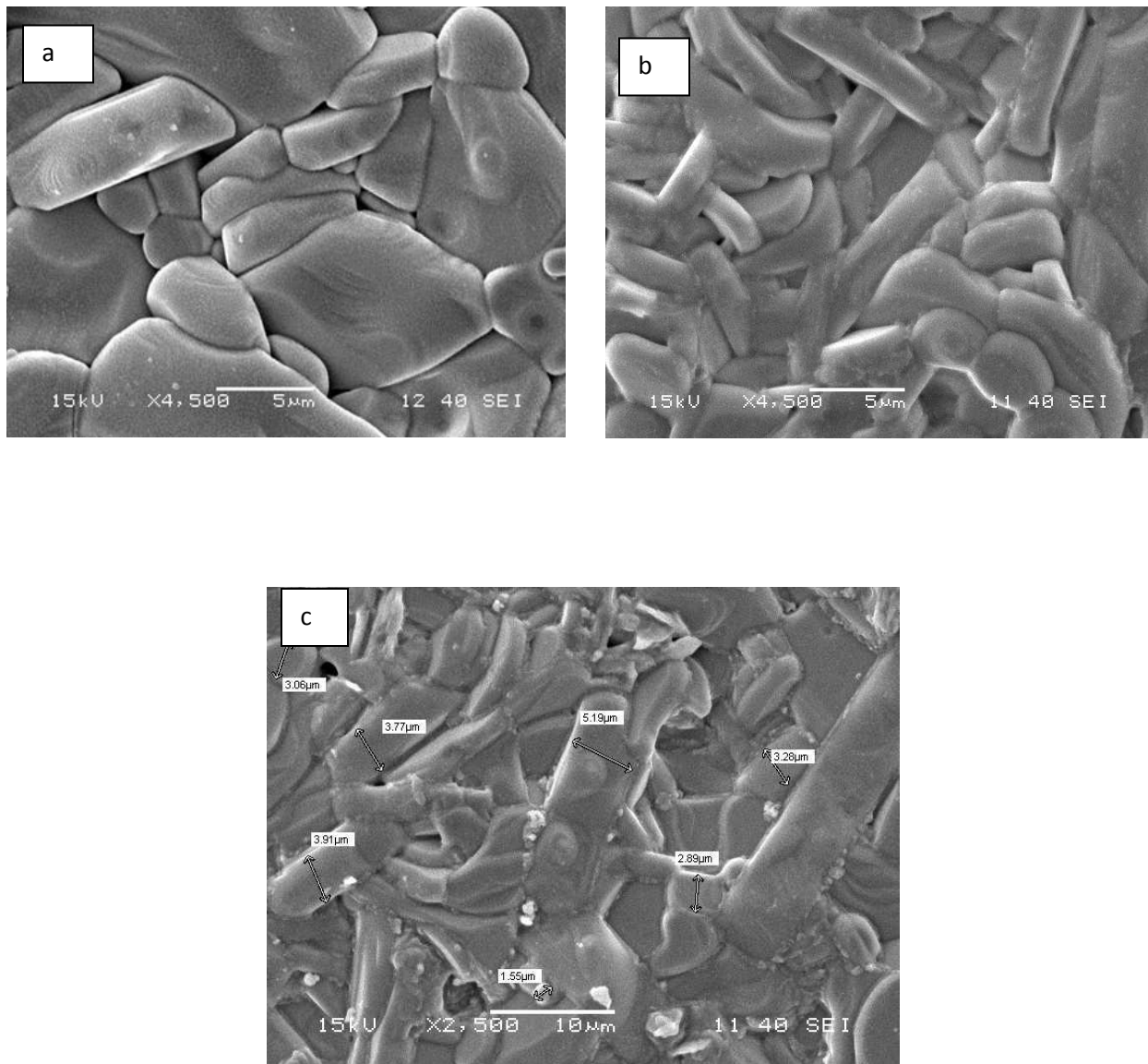


Fig.6. SEM micrographs of YBCO + xBZT composites (x = 0.0, 1.0, 5.0 wt. % marked as a, b, c respectively).

The microstructure characterization i.e., grain-size distribution of the composites as shown in Fig. 6 It gives an idea that the superconductor ferroelectric composites is linked to transport properties. It shows that pristine YBCO sample exhibits large grains randomly oriented in all

directions with size varying from 5 to 15 μm in length. With BZT addition two changes on microstructure are observed, firstly the grain becomes elongated lengthwise, giving rise to rod like structure. Secondly BZT particles are observed sticking to the surface filling up cracks and voids which is evident from fig 6(b). Extra deposition of BZT is observed between grains for 5wt % which may be accounted to excess addition of BZT. White patches of BZT are also observed in fig 6(c).

5. Conclusion

The chemically prepared $\text{BaZr}_{0.1}\text{Ti}_{0.9}\text{O}_3$ having submicron particle size is dispersed in the YBCO matrix is shown in the SEM image. From the R-T plot it is observed that T_c value decreases with increase in $\text{BaZr}_{0.1}\text{Ti}_{0.9}\text{O}_3$ wt. % in the composites and affect the transport property. The pinning properties of BZT can be utilized for enhancement of critical current density of the composite system.

6. References

1. "Solid state physics" – S.O.Pillai
2. "Solid state physics"- Kittel
3. H.Y.Lee, S.I.Kim, Y.C.Lee, Y.P.Hong, Y.H.Park, & K.H.Ko. 13 (2003) 2743
4. A. Mohanta, D. Behera *physica C* 470 (2010) 295-303
5. A. Mohanta and D Behera, *Indian Journal of Physics*. 83:4, 455 (2009)
6. N. C. Mishra, D. Behera, T. Mohanty, K. Patnaik, L. Senapati, O. G. Singh, D. Kanjilal, G. K. Mehta and R. Pinto, *Mod. Phys. Lett. B* 13, 79 (1999)

